Faraday Discussions

Cite this: *Faraday Discuss.*, 2023, **245**, 284

ROYAL SOCIETY OF CHEMISTRY

PAPER

View Article Online
View Journal | View Issue

Searches for bridged bicyclic molecules in space—norbornadiene and its cyano derivatives†

Marie-Aline Martin-Drumel, [a] Jean-Thibaut Spaniol,[a] Helen Hölzel, [b] Marcelino Agúndez,[c] Jose Cernicharo,[c] Kasper Moth-Poulsen [bdef] and Ugo Jacovella *[a]

Received 26th January 2023, Accepted 14th February 2023
DOI: 10.1039/d3fd00016h

The norbornadiene (**NBD**) molecule, C_7H_8, owes its fame to its remarkable photoswitching properties that are promising for molecular solar-thermal energy storage systems. Besides this photochemical interest, **NBD** is a rather unreactive species within astrophysical conditions and it should exhibit high photostability, properties that might also position this molecule as an important constituent of the interstellar medium (ISM)—especially in environments that are well shielded from short-wavelength radiation, such as dense molecular clouds. It is thus conceivable that, once formed, **NBD** can survive in dense molecular clouds and act as a carbon sink. Following the recent interstellar detections of large hydrocarbons, including several cyano-containing ones, in the dense molecular cloud TMC-1, it is thus logical to consider searching for NBD—which presents a shallow but non-zero permanent electric dipole moment (0.06 D)—as well as for its mono- and dicyano-substituted compounds, referred to as **CN-NBD** and **DCN-NBD**, respectively. The pure rotational spectra of **NBD**, **CN-NBD**, and **DCN-NBD** have been measured at 300 K in the 75–110 GHz range using a chirped-pulse Fourier-transform millimetre-wave spectrometer. Of the three species, only **NBD** was previously studied at high resolution in the microwave domain. From the present measurements, the derived spectroscopic constants enable prediction of the spectra of all three species at various rotational temperatures (up to 300 K) in the spectral range mapped at high resolution by current radio observatories. Unsuccessful searches for these molecules were

[a]*Université Paris-Saclay, CNRS, Institut des Sciences Moléculaires d'Orsay, 91405 Orsay, France. E-mail: ugo.jacovella@universite-paris-saclay.fr*
[b]*Department of Chemistry and Chemical Engineering, Chalmers University of Technology, 41296 Gothenburg, Sweden*
[c]*Instituto de Física Fundamental, CSIC, Department of Molecular Astrophysics, Serrano 121, E-28006 Madrid, Spain*
[d]*The Institute of Materials Science of Barcelona, ICMAB-CSIC, Bellaterra, 08193 Barcelona, Spain*
[e]*Catalan Institution for Research & Advanced Studies, ICREA, Pg. Lluís Companys 23, 08010 Barcelona, Spain*
[f]*Department of Chemical Engineering, Universitat Politècnica de Catalunya, EEBE, Eduard Maristany 10–14, 08019 Barcelona, Spain*

† Electronic supplementary information (ESI) available. See https://doi.org/10.1039/d3fd00016h

conducted toward TMC-1 using the QUIJOTE survey, carried out at the Yebes telescope, allowing derivation of the upper limits to the column densities of 1.6×10^{14} cm^{-2}, 4.9×10^{10} cm^{-2}, and 2.9×10^{10} cm^{-2} for **NBD**, **CN-NBD**, and **DCN-NBD**, respectively. Using **CN-NBD** and cyano-indene as proxies for the corresponding bare hydrocarbons, this indicates that—if present in TMC-1—**NBD** would be at least four times less abundant than indene.

Introduction

The hunt for carbon-based molecules in space is a long-standing venture for astrochemists and astronomers.[1] Their identification is mandatory to understand the carbon life cycle at work in extraterrestrial environments and to determine the initial physicochemical conditions in star and planet formation that ultimately led to the conditions for life on Earth.[2] Nowadays, more than 270 gas phase molecular species are known to be present in the interstellar medium (ISM) with ~90% detected by radio astronomy *via* their pure rotational spectral signatures.[3] The detection of these molecules usually results from a collective endeavour within the fields of astronomy, laboratory spectroscopy, and quantum chemistry. The continuous advances in the sensitivity that can be achieved by radio telescopes have led to a large increase in the number of detected molecules within the last 2 years. Conceivably, the culmination of these recent successes is the discovery of numerous aromatics and polycyclic aromatics with an attached –CN function and even one "bare" polycyclic aromatic hydrocarbon (PAH)—indene—using the GOTHAM and QUIJOTE spectral surveys of TMC-1 carried out with the Green Bank and Yebes 40 m telescopes, respectively.[4–10]

The PAH hypothesis[11,12] is now unambiguously confirmed and together with the detection of large carbon cages in different space environments,[13–15] it is strongly tenable that other large carbonaceous systems must exist in space. In general, for molecules to build up large enough densities in space and be detected, they need to be formed efficiently and/or to survive (UV photostability, weak reactivity) long enough to accumulate. A family fulfilling at least the survival criterion is that of diamondoids, which are cage-like, ultra stable, saturated ringed hydrocarbons; the smallest unit being the adamantane ($C_{10}H_{16}$) molecule. Numerous hints allude to the presence of diamondoids in various objects in the universe. Indeed, they possess a strong aptitude for resisting harsh UV radiation[16] and were identified in meteorites[17–19] and in proto-planetary discs.[20] The detection of adamantane or any of its derivatives using radio astronomy, however, remains elusive.[21] From classical synthesis of diamantane ($C_{14}H_{20}$) and larger adamantane clusters ($C_{10+4n}H_{16+4n}$) in Earth laboratories, which typically involves the polymerisation of 2,5-norbornadiene (or 2,2,1-bicycloheptadiene, C_7H_8, hereafter **NBD**; see Zieliński *et al.*[22] and ref. therein), one can foresee **NBD** to be a piece of the complex puzzle generated by the chemical composition of the ISM.

The **NBD** molecule is well known by virtue of its remarkable photoswitching properties showing great promise for molecular solar-thermal energy storage systems.[23] Besides this photochemical interest, **NBD** is a rather nonreactive species by astrophysical standards. It should exhibit high-photostability properties that might also position this molecule as an important constituent of the ISM. **NBD** has its first electronic transition observed around 236 nm, which is

symmetry forbidden and thus extremely weak. The absorption cross section only becomes significant below 200 nm.[24] Under irradiation at 235.7 nm, **NBD** exhibits a fragmentation yield—to form cyclopentadiene and acetylene—of 0.55. The remaining 0.45 yield is the isomerisation to quadricyclane or toluene.[25] Naturally, regions that are well shielded from short-wavelength radiation, such as dense molecular clouds, appear as the most suitable environments to find **NBD**. It is thus conceivable that, once formed, **NBD** can survive in dense molecular clouds and act as a carbon sink.

Because of its broad relevance to many fields, **NBD** has been the subject of several spectroscopic investigations. In the gas phase, electron diffraction and infrared spectroscopy have been employed to determine its structure (see, *e.g.*, ref. 26–28). The electronic spectrum of its cationic counterpart unveiling several interconversion routes on the $C_7H_8^+$ potential energy surface was reported.[29] One gas-phase study examined the photoisomerisation of a charged tagged **NBD** derivative as a function of the excitation wavelength.[30] The pure rotational spectrum of **NBD** (and its isotopologues) has been investigated by Fourier-transform microwave spectroscopy in the 7–17 GHz region.[31,32] These measurements were performed in waveguide cells, with the cells cooled down to −70 °C, hence relatively large quantum number values were probed (up to $J'' = 37$ and $K_a'' = 16$), allowing for the determination of quartic centrifugal distortion constants. Several rovibrational bands were subsequently observed using high-resolution Fourier-transform infrared spectroscopy, providing improved spectroscopic constants using ground-state combination differences owing to a significant increase in observed quantum number values (up to $J'' = 89$ and $K_a'' = 80$).[33] One can expect these constants to allow for reliable predictions of the pure rotational spectrum of **NBD** at higher frequencies than already observed, although no measurements have been reported to date to confirm this. Since many large carbon molecules have recently been detected by radio astronomy at millimetre wavelengths,[9] experimental measurements of **NBD** at these frequencies seem warranted to ensure the accuracy of the spectral predictions.

The shallow permanent electric dipole moment of **NBD** (0.06 D, measured accurately by Stark experiments[31]) implies that a considerable amount of the molecule must be present to be detected. Searching for its cyano derivatives—of much larger permanent dipole moment—may help to overcome this complication. The recent detection of several cyano-substituted molecules[4,6,7] renders the strategy of searching for cyano derivatives extremely tantalising and provides a two-fold piece of information: (i) the cyano derivatives are good trackers of aromatics that own no or weak permanent dipole moments; and (ii) the unexpected large abundance of the found interstellar cyano species informs on the potential chemical role of cyano-bearing molecules in space. Nevertheless, the hardship of reproducing the abundances of these cyano aromatics with current astrochemical models prevents their use as a direct proxy, *i.e.*, the abundance of the non-substituted counterparts cannot be retrieved reliably. Indene is currently the single polycyclic aromatic hydrocarbon for which both the pure hydrocarbon and a cyano-substituted counterpart have been detected in the same source, providing a direct determination of the ratio of their abundance.[34] Even though this observed ratio is reasonably close to the one predicted by computations, the detection of only one of the cyano-derivative isomers still challenges the theory. **NBD** thus appears as a potential highly strained hydrocarbon on which to further

test the proxy hypothesis (*i.e.*, infer the abundance of a non-polar large hydrocarbon based on the interstellar abundance of its cyano derivatives). Literature on the cyano derivatives of **NBD** is rather scarce compared to their bare chromophore and mostly focused on their photoisomerisation properties[35,36]—of relevance to potential new energy storage solutions—and role in Diels–Alder cycloadditions.[37,38] Spectroscopic information on the gaseous compounds is, to the best of our knowledge, limited to a couple of electronic structure investigations.[39,40]

In this paper, we present the pure rotational spectra of **NBD** and two of its mono- and dicyano-substituted compounds, namely bicyclo[2.2.1]hepta-2,5-diene-2-carbonitrile and bicyclo[2.2.1]hepta-2,5-diene-2,3-dicarbonitrile, referred to as **CN-NBD** and **DCN-NBD**, respectively. Measurements were performed at 300 K in the 75–110 GHz range using a chirped-pulse (CP) Fourier-transform millimetre-wave (FTMM) spectrometer. From these measurements, the derived spectroscopic constants are used to predict the spectra of all three species at various rotational temperatures (up to 300 K) in the spectral range in which cold sources are currently mapped at high resolution by radio observatories. Searches for the three species have been undertaken in the 31–40 GHz region on the QUIJOTE line survey of TMC-1.[41] This survey has previously shown the presence of large cyclic molecules, such as indene,[9] which suggests that other large cyclic species, such as **NBD** or its cyano derivatives, could be present as well.

Methods

Sample synthesis

NBD was purchased from Sigma-Aldrich (≥97% purity) and used without further purification. **CN-NBD** and **DCN-NBD** were synthesised at Chalmers University.

CN-NBD was prepared following a procedure adapted from the literature;[42,43] the corresponding scheme is displayed is Fig. S1 in the ESI†. Briefly, propargyl alcohol (1.11 g; 19.8 mmol) was combined with cyclopentadiene (1.32 g, 20 mmol) and hydroquinone (a few crystals) in a 20 mL vial, suitable for microwave reactions, and sealed. The mixture was heated to 170 °C for 8 h. The crude product was purified *via* flash column chromatography in 100% dichloromethane. The resulting product, (±)-2-hydroxymethylbicyclo[2.2.1]-hepta-2,5-diene, is an oil and was obtained in a 7.8% yield (0.19 g, 1.55 mmol). ^{1}H NMR data (Fig. S2†) are in accordance with literature data.[42] (±)-2-Hydroxymethylbicyclo[2.2.1]-hepta-2,5-diene (0.19 g, 1.55 mmol) was then combined with CH_3CN (4 mL), H_2O (0.5 mL), TEMPO (12 mg, 77 mmol), NH_4OAc (0.475 g, 6.16 mmol), and $PhI(OAc)_2$ (1.06 g, 3.3 mmol), and stirred at room temperature for 1 h. Dichloromethane was added to the reaction mixture and the phases were separated. The aqueous phase was extracted with dichloromethane (repeated three times) and the solvent was evaporated. The crude product was purified using flash column chromatography in 100% petroleum spirit. The pure product, **CN-NBD**, was isolated in 11% yield (20 mg, 0.17 mmol). NMR data are in accordance with literature data.[44]

The synthesis for **DCN-NBD** was carried out according to literature procedures (Fig. S3†); ^{1}H and ^{13}C NMR characterisation data (Figs. S4 and S5†) are in accordance with the literature.[45,46]

Both samples were stored at −80 °C until their investigation at the University of Paris-Saclay.

Quantum chemical calculations

Calculations were performed using the Gaussian 16 suite of electronic structure programs.[47] Geometry optimisation and harmonic frequency analysis have been carried out at the ωB97X-D/cc-pVQZ level of theory,[48–50] a level that provides very reliable spectroscopic parameters for the spectral analysis of rigid molecules (dipole moment projections, rotational constants, and quartic centrifugal distortion constants).[51,52]

Millimetre-wave measurements

CP-FTMM measurements were performed in the 75–110 GHz spectral range using a commercial CP spectrometer from BrightSpec. Vapour pressure of each sample, typically of the order of 3 μbar, was introduced into a ∼60 cm-long cell terminated by two PTFE windows. A slow flow was ensured by a turbomolecular pump (Pfeiffer, HiCube 80) to maintain stable pressure conditions during the acquisition and prevent cell outgassing. Spectra were recorded in the standard high dynamic range mode of the instrument consisting of a segmented acquisition approach with 30 MHz-wide segments. Excitation pulses of 0.5 μs (the longest possible in this mode of acquisition), 0.25 μs, and 0.1 μs length were found to maximise the signals of **NBD**, **CN-NBD**, and **DCN-NBD**, respectively. These decreasing values are consistent with the increasing permanent dipole moment value of the species—since molecules with lower dipole moments usually require a longer excitation pulse to achieve the highest molecular signal. The final CP spectra were obtained *via* the Fourier transform of 4 μs of the free induction decay, after applying a Blackmann–Harris filter. The spectra were averaged over 1 million, 640 thousand, and 500 thousand frames for **NBD**, **CN-NBD**, and **DCN-NBD**, respectively (2 to 1 h of acquisition time based on sample availability).

Results and discussion

Spectroscopic considerations

Cartesian coordinates of the optimised equilibrium structures can be found in Tables S1–S3 in the ESI.† The associated molecular representations of the three molecules are shown in Fig. 1. **NBD** has C_{2v} point group symmetry and possesses a small permanent dipole moment of 0.06 Debye along the *c*-axis of inertia (where the axis is going through the centre of the C_6H_6 ring and the carbon of the CH_2 moiety). **CN-NBD** has C_1 point group symmetry and its permanent dipole moment has projections along the three axes of inertia, with values of 4.67 Debye, 0.77 Debye, and 0.22 Debye along the *a*-, *b*-, and *c*-axis, respectively (the *a*-axis is parallel to the –CN bond). Finally, **DCN-NBD** has C_s point group symmetry and exhibits projections of its permanent dipole moment of 6.44 Debye and 0.86 Debye along the *a*- and *c*-axis of inertia (the *a* axis is perpendicular to the plane containing the two –CN bonds). Projections of the three molecular structures onto the three inertial planes, performed using the PMIFST software developed by Z. Kisiel,[53] are proposed in Fig. S6 in the ESI.† All three species are asymmetric top rotors with asymmetry parameters κ taking values of −0.2203,[31] −0.9426, and 0.0784, respectively. **NBD** possesses four pairs of exchangeable H nuclei with respect to the C_2-axis resulting in a statistical weight for the *ortho* : *para* levels of 17 : 15. This ratio, very close to unity, did not result in any tangible intensity

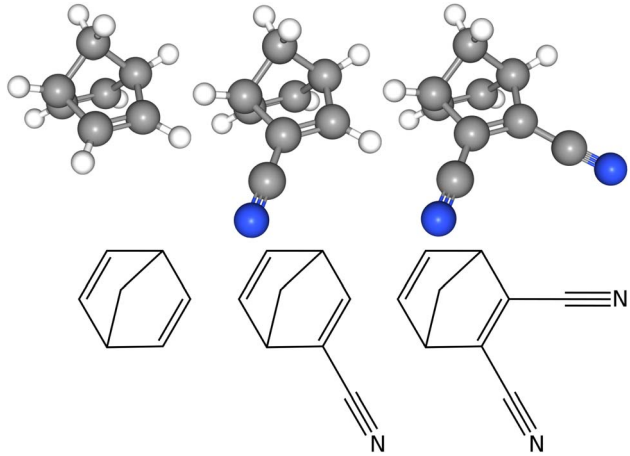

Fig. 1 Molecular representations of **NBD**, **CN-NBD**, and **DCN-NBD** (from left to right).

difference on the experimental spectrum but was nonetheless taken into account for the spectral predictions.

Rotational analysis

Experimental assignments have been performed using the PGOPHER software by exploiting Loomis–Wood diagrams.[54] PGOPHER was also used for spectral simulations. The SPFIT/SPCAT suite of programs[55] was used to adjust the rotational constants of all three species using a Watson A-reduced Hamiltonian in the I^r representation.

For **NBD**, literature pure rotation data[31] (25 transitions) and ground-state combination differences (GSCD) from rovibrational data[33] (369 GSCD/196 wavenumbers) were fitted together allowing for efficient searches at millimetre wavelengths. Both datasets were weighted according to their expected accuracy, *i.e.*, 1 kHz for data from Vogelsanger and Bauder[31] and 0.0001 cm^{-1} to 0.0003 cm^{-1} (~3–9 MHz) for GCSD from Sams and Blake.[33] GCSD are provided in MHz in ref. 33 but we favoured here wavenumber units in order to access individual root mean square values for the two datasets, as conventionally done using SPFIT. To reproduce these datasets at their experimental accuracy, all three rotational constants and five quartic centrifugal distortion parameters were adjusted. The resulting parameters are reported in Table 1 and are in excellent agreement with those reported by Sams and Blake.[33] The only difference is that we chose not to adjust the sextic centrifugal distortion parameter h_K in favour of a more constrained fit. All parameters are also in excellent agreement with those predicted from the calculations performed in this study. Using these reliable constants, spectroscopic assignments of the millimetre-wave spectrum of **NBD** were straightforward, with no notable divergence of the prediction. In total, 94 transitions (79 different frequencies) involving $J'' \leq 16$ and $K_a'' \leq 11$ were assigned on the spectrum. Frequency accuracy is estimated to be 30 kHz. These transitions were fitted together with the literature and GSCD data; the adjusted spectroscopic parameters are reported in Table 1. All transitions are reproduced at their

Table 1 Rotational constants and quartic centrifugal distortion constants (in MHz) of NBD, CN-NBD, and DCN-NBD. Predictions (Pred.) result from the ωB97X-D/cc-pVQZ calculations with Bayesian correction for the rotational constants;[51] harmonic equilibrium values are reported for the centrifugal distortion parameters. For NBD, values derived from the refit of the literature data (Lit.) are reported together with the combined fit from this work (TW). All adjusted parameters are reported with 1σ uncertainties expressed in the unit of the last digit in parentheses. The value in square brackets is fixed to the calculated value. Relevant fit parameters are reported at the bottom of the table

		NBD			CN-NBD		DCN-NBD	
Parameter		Pred.	Lit.[a]	TW	Pred.	TW	Pred.	TW
A		4279.20	4273.62825(11)	4273.628151(89)	3829.02	3831.6473(15)	1519.59	1524.6688(45)
B		3590.28	3610.30044(10)	3610.300350(86)	1309.06	1316.14694(25)	1180.74	1186.9614(30)
C		3176.64	3186.43725(10)	3186.437158(87)	1235.56	1241.76251(23)	788.07	791.81703(12)
Δ_J	$\times 10^3$	0.3284	0.33376(21)	0.33379(21)	0.05950	0.063035(52)	0.3917	0.10090(83)
Δ_{JK}	$\times 10^3$	−0.07030	−0.07239(71)	−0.07226(70)	0.5917	0.62671(24)	−1.2814	−0.3979(45)
Δ_K	$\times 10^3$	0.2679	0.26745(61)	0.26725(59)	0.08843	0.0533(24)	0.9067	[0.9067]
δ_J	$\times 10^3$	0.004560	0.004777(82)	0.004790(80)	0.00308	0.003530(44)	0.1122	0.04124(42)
δ_K	$\times 10^3$	0.08956	0.09221(77)	0.09206(76)	0.06219	0.0805(53)	−1.0833	−0.08482(41)
N/n[b]			394/221	438/300		1067/626		761/389
$J''_{\max}$, $K''_{a\,\max}$			89, 80	89, 80		74, 40		67, 21
RMS[c]			0.00079	0.027		0.051		0.026
IR RMS[d]			0.00014	0.00014				
σ[e]			1.03	1.03		0.96		0.87

[a] Refit of the literature data: pure rotation from Vogelsanger and Bauder[31] (in MHz) and ground-state combination differences from Sams and Blake[33] (in cm^{-1}). [b] Number of lines (N) and number of lines with different frequencies (n), unitless. [c] Root mean square of the microwave data, in MHz. [d] Root mean square of the infrared data, in cm^{-1}. [e] Weighted standard deviation, unitless.

expected accuracy with a final weighted standard deviation of 1.03. The addition of the millimetre-wave transitions allows for a slight, but not substantial, refinement of the parameters (Table 1). Nevertheless, accurate experimental frequencies of **NBD** are now available in the millimetre-wave domain, and spectral predictions in the range not covered yet in the laboratory, 17–75 GHz, should be extremely reliable. Frequency extrapolation always requires more caution, although for a molecule as rigid as **NBD**—only 8 parameters are required to reproduce 300 different frequencies with transitions involving J and K_a as high as 89 and 80, respectively—these are expected to be trustworthy as well.

For the two other species studied here, **CN-NBD** and **DCN-NBD**, since no literature data was available on the spectroscopic constants, spectral searches were initiated using the rotational constants derived from the calculated equilibrium structure. To more accurately predict the rotational constants in $v = 0$, the equilibrium A, B, and C values were scaled using the Bayesian correction factor recommended for the ωB97X-D/cc-pVQZ level of calculations (0.9866).[51] These predicted constants are reported in Table 1 (the equilibrium A_e, B_e, and C_e values are available in Table S4 in the ESI†). In both cases, the predictions allowed for a straightforward assignment of the pure rotational transitions.

For **CN-NBD**, a-type R-branch transitions were assigned first, owing to the large projection of the permanent dipole moment along that axis ($\mu_a = 4.67$). In total, 863 transitions (524 different frequencies) involving quantum numbers up to $J'' = 42$ and $K_a'' = 40$ were assigned with the frequency accuracy estimated to be 30 kHz. These transitions allowed for the determination of the rotational constants and quartic centrifugal distortion constants, with the exception of Δ_K (which is typical of a fit involving only a-type transitions). After this first iteration of assignments, b-type Q-branch transitions were identified on the spectrum. These transitions are about 30 times weaker than the a-type ones, in qualitative agreement with what is expected from the squared ratio of the dipole-moment projections $[(\mu_a/\mu_b)^2 = 36]$. 204 of these transitions (102 different frequencies) involving $J'' \leq 74$ and $K_a'' \leq 20$ were assigned. These lines exhibit a lower signal-to-noise ratio than the a-type ones and their frequency uncertainty is consequently estimated to be 100 kHz. No a-type Q-branch or b-type R-branch transitions were assigned, nor were any c-type ones (they are mostly overlapping with stronger b-type transitions). The addition of the b-type transitions to the fit enabled the determination of the Δ_K parameter (Table 1). No additional distortion parameter was required to reproduce the data at their experimental accuracy (the final weighted standard deviation is 0.96)—not even J-dependant ones, even though high J values are observed—which highlights the rigidity of the molecule. The adjusted set of parameters is in excellent agreement with the predicted one, with the relative error on the rotational constants on the order of 0.5% or better (against 1–1.25% for the pure equilibrium values), which is consistent with what has previously been observed using the Bayesian correction.[52] The experimentally-derived centrifugal distortion constants are also in good agreement with the calculations, both in sign and order of magnitude. Fig. 2 shows a comparison between portions of the experimental spectrum of **CN-NBD** and the simulation obtained using the optimised parameters.

Finally, for **DCN-NBD**, 761 a-type R-branch transitions (389 different frequencies) with $J'' \leq 67$ and $K_a'' \leq 21$ have been assigned. No b-type transitions were assigned because these weaker features are overlapping with the a-type

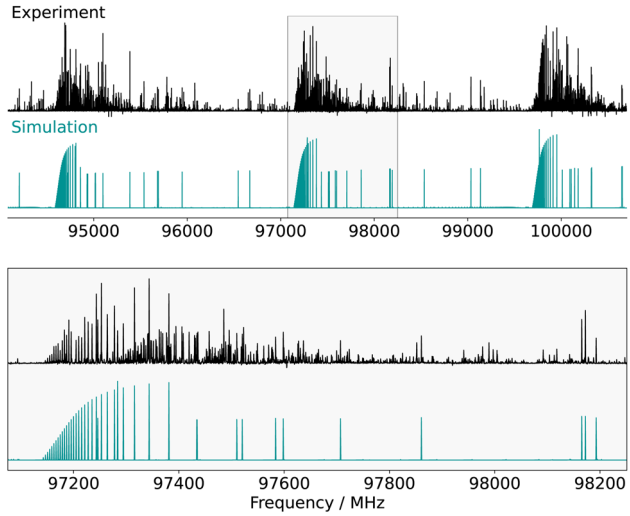

Fig. 2 Portions of the experimental spectrum (in black) of **CN-NBD** recorded using the CP-FTMM spectrometer and comparison with a 300 K simulation performed using the rotational constants derived from the spectral analysis (in green). The bottom panel shows the zoomed-in regions of the spectra around the $^{Q}R(J'' = 37)$ transition; the corresponding spectral window is highlighted by a grey area on the top panel. Transitions on the experimental spectrum not reproduced on the simulation arise from vibrational satellites (pure rotation in excited vibrational states) not investigated in this work.

transitions. The assigned transitions, of expected frequency accuracy of 30 kHz, have enabled the adjustment of the rotational and quartic centrifugal distortion constants of the molecule (Table 1). The Δ_K parameter could not be adjusted and was thus fixed to the calculated value. The derived rotational constants are again in excellent agreement with the prediction (with relative errors on the order of 0.5% or better). The centrifugal distortion parameters are further away from the calculated values than for the other species (by a factor of 3 to 10), while agreeing in sign, but fixing some distortion parameters (*e.g.*, δ_K, which is showing the worse agreement) to the calculated values does not allow a satisfactory fit to be obtained. Overall, all transitions are reproduced at their expected accuracy with a final root-mean-square of 26 kHz, corresponding to a weighted standard deviation close to unity.

All files relevant to the assignment and fit (linelists, parameters, and fit results) are available in the ESI† as ASCII files.

Astronomical implications and interstellar searches

Using the spectroscopic parameters determined for the three species in this study, reliable spectral predictions can be obtained for frequencies up to 110 GHz and temperatures up to 300 K (so as to simulate transitions involving the same range of quantum numbers as those observed experimentally). Frequency and/or temperature extrapolation may be feasible as well since the three species appear particularly rigid, although the accuracy of such predictions is hard to estimate. Catalogues of the frequencies at 10 K have been generated for the three molecules

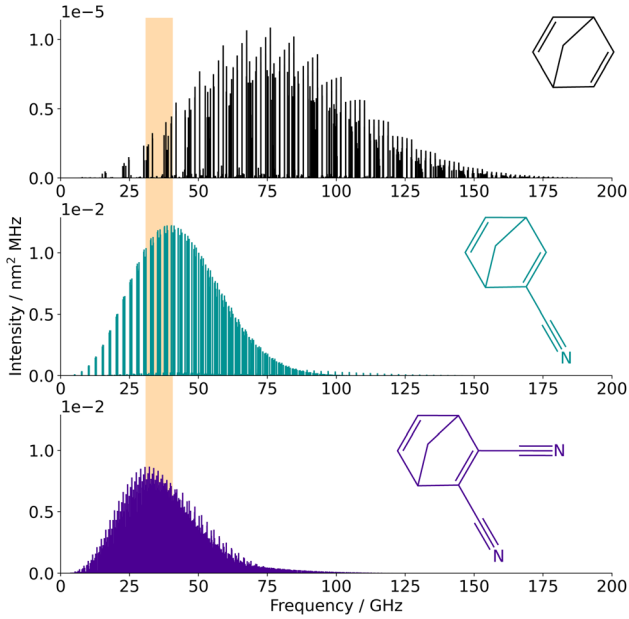

Fig. 3 Simulated spectra of **NBD**, **CN-NBD**, and **DCN-NBD** (from top to bottom) at 10 K. The orange area is the spectral regions where features of these species were searched for on the QUIJOTE survey.

using the SPCAT program and the partition functions reported in Table S5 in the ESI† (also generated using SPCAT); the corresponding traces are shown in Fig. 3. At this temperature, the strongest transitions of **NBD** lie around 75 GHz while the spectrum of the two –CN substituted species is shifted to lower frequencies (because of their heavier weight) with an optimum region for interstellar searches between ∼25 GHz and ∼50 GHz.

The frequency predictions of **NBD**, **CN-NBD**, and **DCN-NBD** were used to search for these three species toward the starless core TMC-1 using the QUIJOTE line survey of this source that is being carried out with the Yebes 40 m telescope.[41] Currently, the QUIJOTE data cover observing sessions from November 2019 to November 2022, and amount to a total on-source telescope time of 758 h. The

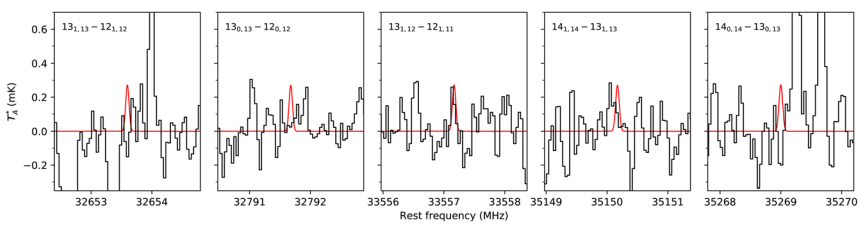

Fig. 4 QUIJOTE data at the position of some of the lines of **CN-NBD** predicted to be the most intense. Red traces are the synthetic line profiles calculated assuming a rotational temperature of 10 K, a line width of 0.6 km s^{-1}, and a column density equal to the 3σ upper limit derived, *i.e.*, 4.9 × 10^{10} cm^{-2}.

antenna temperature noise level is around 0.1 mK in the 31–40 GHz region and somewhat higher at frequencies above 40 GHz. We thus carried out the search for **NBD** and its cyano derivatives focusing on the low-frequency data of the QUIJOTE survey (region highlighted in orange in Fig. 3). At the current sensitivity level of the data, we do not detect the lines predicted to be the most intense in this frequency region for neither **NBD**, **CN-NBD**, nor **DCN-NBD**. Assuming a rotational temperature of 10 K and line width of 0.6 km s^{-1}, as found for indene,[9] we derive 3σ upper limits to the column densities of 1.6×10^{14} cm^{-2} for **NBD**, 4.9×10^{10} cm^{-2} for **CN-NBD**, and 2.9×10^{10} cm^{-2} for **DCN-NBD**. Fig. 4 illustrates the non-detection of the most intense lines of **CN-NBD** assuming the aforementioned conditions. The upper limit derived for **NBD** is quite high and thus not very informative due to the very low dipole moment of this molecule. For comparison, the column density derived for indene, a molecule that is also weakly polar, is 1.6×10^{13} cm^{-2}.[9] On the other hand, the upper limit imposed on the monocyano derivative, which is very polar, is much more informative. For comparison, the column density inferred for the monocyano derivative of indene is 2.1×10^{11} cm^{-2}.[34] If the abundance ratio between the monocyano derivative and the parent hydrocarbon behaves similarly for indene and **NBD**, then **NBD**—if present in TMC-1—is less abundant than indene by a factor of at least four.

Conclusions

The pure rotational spectra of **NBD**, **CN-NBD**, and **DCN-NBD** have been investigated at room temperature by CP-FTMM spectroscopy in the 75–110 GHz range allowing for a refinement of the spectroscopic constants of **NBD** and the first experimental determination of those of **CN-NBD** and **DCN-NBD**. Using these constants, transitions of the three molecules have been searched for, unsuccessfully, toward TMC-1 using the QUIJOTE survey. Upper limits to the column density of each species have been derived.

Conflicts of interest

There are no conflicts to declare.

Acknowledgements

The work at ISMO was performed using HPC resources from the "Mésocentre" computing center of CentraleSupélec and École Normale Supérieure Paris-Saclay supported by CNRS and Région Île-de-France (**https://mesocentre.centralesupelec.fr/**). It has also been supported by the Région Ile-de-France, through DIM-ACAV+, from the Agence Nationale de la Recherche (ANR-19-CE30-0017-01), and from the Programme National "Physique et Chimie du Milieu Interstellaire" (PCMI) of CNRS/INSU with INC/INP co-funded by CEA and CNES. The work at Chalmers was funded by the European Research Council (ERC) under grant agreement CoG, PHOTHERM – 101002131, the Catalan Institute of Advanced Studies (ICREA), and the European Union's Horizon 2020 Framework Programme under grant agreement no. 951801. We thank Anders Lennartsson for his help with the synthesis of **CN-NBD**.

Notes and references

1 C. S. Hansen, E. Peeters, J. Cami and T. W. Schmidt, *Commun. Chem.*, 2022, **5**, 94.
2 S. A. Sandford, M. Nuevo, P. P. Bera and T. J. Lee, *Chem. Rev.*, 2020, **120**, 4616–4659.
3 B. A. McGuire, *Astrophys. J., Suppl. Ser.*, 2022, **259**, 30.
4 B. A. McGuire, A. M. Burkhardt, S. Kalenskii, C. N. Shingledecker, A. J. Remijan, E. Herbst and M. C. McCarthy, *Science*, 2018, **359**, 202–205.
5 A. M. Burkhardt, R. A. Loomis, C. N. Shingledecker, K. L. K. Lee, A. J. Remijan, M. C. McCarthy and B. A. McGuire, *Nat. Astron.*, 2021, **5**, 181–187.
6 M. C. McCarthy, K. L. K. Lee, R. A. Loomis, A. M. Burkhardt, C. N. Shingledecker, S. B. Charnley, M. A. Cordiner, E. Herbst, S. Kalenskii, E. R. Willis, et al., *Nat. Astron.*, 2021, **5**, 176–180.
7 K. L. K. Lee, P. B. Changala, R. A. Loomis, A. M. Burkhardt, C. Xue, M. A. Cordiner, S. B. Charnley, M. C. McCarthy and B. A. McGuire, *Astrophys. J., Lett.*, 2021, **910**, L2.
8 B. A. McGuire, R. A. Loomis, A. M. Burkhardt, K. L. K. Lee, C. N. Shingledecker, S. B. Charnley, I. R. Cooke, M. A. Cordiner, E. Herbst, S. Kalenskii, et al., *Science*, 2021, **371**, 1265–1269.
9 J. Cernicharo, M. Agúndez, C. Cabezas, B. Tercero, N. Marcelino, J. R. Pardo and P. de Vicente, *Astron. Astrophys.*, 2021, **649**, L15.
10 A. M. Burkhardt, K. L. K. Lee, P. B. Changala, C. N. Shingledecker, I. R. Cooke, R. A. Loomis, H. Wei, S. B. Charnley, E. Herbst, M. C. McCarthy, et al., *Astrophys. J., Lett.*, 2021, **913**, L18.
11 L. Allamandola, A. Tielens and J. Barker, *Astrophys. J., Suppl. Ser.*, 1989, **71**, 733–775.
12 S. Schlemmer, D. Cook, J. Harrison, B. Wurfel, W. Chapman and R. Saykally, *Science*, 1994, **265**, 1686–1689.
13 B. Foing and P. Ehrenfreund, *Nature*, 1994, **369**, 296–298.
14 J. Cami, J. Bernard-Salas, E. Peeters and S. E. Malek, *Science*, 2010, **329**, 1180–1182.
15 E. K. Campbell, M. Holz, D. Gerlich and J. P. Maier, *Nature*, 2015, **523**, 322–323.
16 W. C. Saslaw and J. E. Gaustad, *Nature*, 1969, **221**, 160–162.
17 R. S. Lewis, T. Ming, J. F. Wacker, E. Anders and E. Steel, *Nature*, 1987, **326**, 160–162.
18 R. S. Lewis, E. Anders and B. T. Draine, *Nature*, 1989, **339**, 117–121.
19 E. Anders and E. Zinner, *Meteoritics*, 1993, **28**, 490–514.
20 A. P. Jones, *Astron. Astrophys.*, 2022, **665**, A21.
21 O. Chitarra, M.-A. Martin-Drumel, Z. Buchanan and O. Pirali, *J. Mol. Spectrosc.*, 2021, **378**, 111468.
22 A. Zieliński, X. Marset, C. Golz, L. M. Wolf and M. Alcarazo, *Angew. Chem., Int. Ed.*, 2020, **59**, 23299–23305.
23 M. Quant, A. Lennartson, A. Dreos, M. Kuisma, P. Erhart, K. Börjesson and K. Moth-Poulsen, *Chem. - Eur. J.*, 2016, **22**, 13265–13274.
24 B. O. Roos, M. Merchan, R. McDiarmid and X. Xing, *J. Am. Chem. Soc.*, 1994, **116**, 5927–5936.
25 B. Roquitte, *J. Phys. Chem.*, 1965, **69**, 2475–2477.

26 A. Yokozeki and K. Kuchitsu, *Bull. Chem. Soc. Jpn.*, 1971, **44**, 2356–2363.
27 I. W. Levin and W. Harris, *Spectrochim. Acta, Part A*, 1973, **29**, 1815–1834.
28 R. A. Shaw, C. Castro, R. Dutler, A. Rauk and H. Wieser, *J. Chem. Phys.*, 1988, **89**, 716–731.
29 U. Jacovella, G. da Silva and E. J. Bieske, *J. Phys. Chem. A*, 2019, **123**, 823–830.
30 U. Jacovella, E. Carrascosa, J. T. Buntine, N. Ree, K. V. Mikkelsen, M. Jevric, K. Moth-Poulsen and E. J. Bieske, *J. Phys. Chem. Lett.*, 2020, **11**, 6045–6050.
31 B. Vogelsanger and A. Bauder, *J. Mol. Spectrosc.*, 1988, **130**, 249–257.
32 G. Knuchel, G. Grassi, B. Vogelsanger and A. Bauder, *J. Am. Chem. Soc.*, 1993, **115**, 10845–10848.
33 R. L. Sams and T. A. Blake, *J. Mol. Spectrosc.*, 2020, **373**, 111354.
34 M. L. Sita, P. B. Changala, C. Xue, A. M. Burkhardt, C. N. Shingledecker, K. L. Kelvin Lee, R. A. Loomis, E. Momjian, M. A. Siebert, D. Gupta, E. Herbst, A. J. Remijan, M. C. McCarthy, I. R. Cooke and B. A. McGuire, *Astrophys. J., Lett.*, 2022, **938**, L12.
35 Y. Harel, A. W. Adamson, C. Kutal, P. A. Grutsch and K. Yasufuku, *J. Phys. Chem.*, 1987, **91**, 901.
36 F. Hemauer, U. Bauer, L. Fromm, C. Weiss, A. Leng, P. Bachmann, F. Duell, J. Steinhauer, V. Schwaab, R. Grzonka, A. Hirsch, A. Gorling, H.-P. Steinrueck and C. Papp, *ChemPhysChem*, 2022, **23**, e202200199.
37 E. Dalkilic and A. Dastan, *Tetrahedron*, 2015, **71**, 1966–1970.
38 H. Abdullah, R. Tia and E. Adei, *J. Phys. Org. Chem.*, 2021, **34**, e4259.
39 T. Kobayashi, Z. Yoshida, Y. Asako, S. Miki and S. Kato, *J. Am. Chem. Soc.*, 1987, **109**, 5103.
40 K. N. Houk, N. G. Rondan, M. N. Paddon-Row, C. W. Jefford, P. T. Huy, P. D. Burrow and K. D. Jordan, *J. Am. Chem. Soc.*, 1983, **105**, 5563.
41 J. Cernicharo, M. Agúndez, R. I. Kaiser, C. Cabezas, B. Tercero, N. Marcelino, J. R. Pardo and P. de Vicente, *Astron. Astrophys.*, 2021, **652**, L9.
42 C. Tanyeli, G. Çelikel and İ. M. Akhmedov, *Tetrahedron: Asymmetry*, 2001, **12**, 2305–2308.
43 J.-M. Vatèle, *Synlett*, 2014, **25**, 1275–1278.
44 W. Adam, L. Pasquato, B. Will and O. D. Lucchi, *Chem. Ber.*, 1987, **120**, 531–535.
45 O. Diels and K. Alder, *Justus Liebigs Ann. Chem.*, 1931, **490**, 236–242.
46 H. Taniguchi, T. Ikeda, Y. Yoshida and E. Imoto, *Bull. Chem. Soc. Jpn.*, 1977, **50**, 2694–2699.
47 M. J. Frisch, G. W. Trucks, H. B. Schlegel, G. E. Scuseria, M. A. Robb, J. R. Cheeseman, G. Scalmani, V. Barone, G. A. Petersson, H. Nakatsuji, X. Li, M. Caricato, A. V. Marenich, J. Bloino, B. G. Janesko, R. Gomperts, B. Mennucci, H. P. Hratchian, J. V. Ortiz, A. F. Izmaylov, J. L. Sonnenberg, D. Williams-Young, F. Ding, F. Lipparini, F. Egidi, J. Goings, B. Peng, A. Petrone, T. Henderson, D. Ranasinghe, V. G. Zakrzewski, J. Gao, N. Rega, G. Zheng, W. Liang, M. Hada, M. Ehara, K. Toyota, R. Fukuda, J. Hasegawa, M. Ishida, T. Nakajima, Y. Honda, O. Kitao, H. Nakai, T. Vreven, K. Throssell, J. A. Montgomery Jr, J. E. Peralta, F. Ogliaro, M. J. Bearpark, J. J. Heyd, E. N. Brothers, K. N. Kudin, V. N. Staroverov, T. A. Keith, R. Kobayashi, J. Normand, K. Raghavachari, A. P. Rendell, J. C. Burant, S. S. Iyengar, J. Tomasi, M. Cossi, J. M. Millam, M. Klene, C. Adamo,

R. Cammi, J. W. Ochterski, R. L. Martin, K. Morokuma, O. Farkas, J. B. Foresman and D. J. Fox, *Gaussian 16 Revision A.01*, 2016.
48 J.-D. Chai and M. Head-Gordon, *Phys. Chem. Chem. Phys.*, 2008, **10**, 6615.
49 T. H. Dunning, *J. Chem. Phys.*, 1989, **90**, 1007–1023.
50 D. E. Woon and T. H. Dunning, *J. Chem. Phys.*, 1993, **98**, 1358–1371.
51 K. L. K. Lee and M. McCarthy, *J. Phys. Chem. A*, 2020, **124**, 898–910.
52 Z. Buchanan, K. L. K. Lee, O. Chitarra, M. C. McCarthy, O. Pirali and M.-A. Martin-Drumel, *J. Mol. Spectrosc.*, 2021, **377**, 111425.
53 Z. Kisiel, *Spectroscopy from Space*, Springer, Dordrecht, Netherlands, 2001, pp. 91–106.
54 C. M. Western, *J. Quant. Spectrosc. Radiat. Transfer*, 2017, **186**, 221–242.
55 H. M. Pickett, *J. Mol. Spectrosc.*, 1991, **148**, 371–377.